Clays and Clay Minerals, Vol. 50, No. 2, 145–156, 2002.

ORIGIN OF ALLOPHANE AND RETARDATION OF PEBBLE WEATHERING IN QUATERNARY MARINE TERRACE DEPOSITS

GI YOUNG JEONG[1,*], JIN HAN BAE[1] AND CHANG SIK CHEONG[2]

[1] Department of Earth and Environmental Sciences, Andong National University, Andong 760-749, South Korea
[2] Isotope Research Team, Korea Basic Science Institute, Taejon 305-333, South Korea

Abstract—Quaternary marine terrace deposits consisting of gravels interbedded with thin sandy gravel layers have been subjected to subaerial weathering. Restricted to the sandy gravel layers, allophane gel either replaced bytownite sands to form a pseudomorph or coated the pebbles. The allophane has an average Al/Si atomic ratio of 1.5 with 45% H_2O. The sandy gravels were originally rich in bytownite (av. An_{86}) sands derived from underlying Tertiary basaltic lapilli tuff. The highly soluble and aluminous bytownite favored the formation of allophane. In the sandy gravel layers, pebbles coated with allophane gel were almost fresh whereas those in the gravel layers were highly weathered to form halloysite-rich clays. Allophane gels acted as a somewhat impermeable geochemical barrier impeding a mineral-water reaction in the bytownite-rich sandy gravel layers and thus significantly retarding pebble weathering, while prolonged weathering in the gravel layers resulted in the severe decomposition of pebbles. Bytownite protected the pebbles against weathering, implying that minor soluble minerals might be one of the factors in the natural variation of the weathering rates of rocks and sediments.

Key Words—Allophane, Bytownite, Gravel, Marine Terrace, Weathering.

INTRODUCTION

Allophane and imogolite, amorphous to very poorly crystalline aluminosilicates, occur in diverse geological environments from weathering to hydrothermal activity (Gaines *et al*., 1997). In surface environments, the major occurrences are Andisols from volcanic ash and Spodosols underlying humid cool forest (Wada, 1989), but they are rarely reported from unconsolidated Quaternary sedimentary deposits which are parent materials for productive soils. Feijtel *et al.* (1989), Veldkamp *et al*. (1990), Jongmans *et al.* (1993), and van Oort *et al.* (1994) studied the soils developed on the Quaternary Allier river terrace deposits in France. They described isotropic clay coatings that were interpreted to be amorphous aluminosilicates, but could not identify the mineral species despite careful microscopic investigation. Although the amorphous aluminosilicates in soils are commonly identified by acid-oxalate extraction (Parfitt and Kimble, 1989) and their characteristic particle shape (Henmi and Wada, 1976), their formation from parent materials can be observed directly by the micromorphological, optical and microchemical analysis of thin-sections. Jongmans *et al.* (1994, 1995, 2000) observed coatings and infillings of allophane and imogolite in Andisols.

A number of raised marine terraces are distributed along the southeastern coast of Korea (Lee, 1985). Gravel deposits of marine terraces are subjected to weathering after subaerial exposure. Since materials for absolute age-dating, *e.g.* charcoal, sea shell and coral, are scarce, the degree of weathering of sediments could be used to establish the relative ages of terraces. Soil profiles have been used previously to establish the relative ages and to correlate marine terrace deposits (Langley-Turnbaugh and Bockheim, 1997; Bockheim *et al*., 1992). During our study of weathering of the terrace deposits, we found optically isotropic clays cementing pebbles and sands, and studied how they impeded weathering of the pebbles. This paper reports the occurrences, mineralogical properties, and formation process of the isotropic clays using mainly micromorphological and microchemical methods, and discusses their influence on the weathering of the pebbles.

OCCURRENCE OF WEATHERED MARINE TERRACE DEPOSITS

The study site is located on the coast of Suryum-ri, Kyongju-si (Figure 1). The regional geology consists of Cretaceous granite, arkosic sandstones, hornfels, Tertiary basic volcanics, conglomerates and unconsolidated Quaternary sediments. There are three raised Quaternary marine terraces at altitudes 3–5 m, 10–15 m and 45–55 m covered with gravels (Lee *et al*., 1999). The main object of this study is the uppermost terrace deposit (Figure 1). Lee (1985) assumed the sedimentation age of this deposit to be Early Pleistocene on the basis of paleomagnetic data of colluvium overlying terrace deposits and correlation between terrace elevations and the global eustatic sea-level change curve. In contrast, Kwon *et al.* (1999) reported the optically stimulated luminescence (OSL) ages ranging from 32 to 58 ka for the deposit and raised a question as to the simple correlation by present

* E-mail address of corresponding author:
jearth@andong.ac.kr

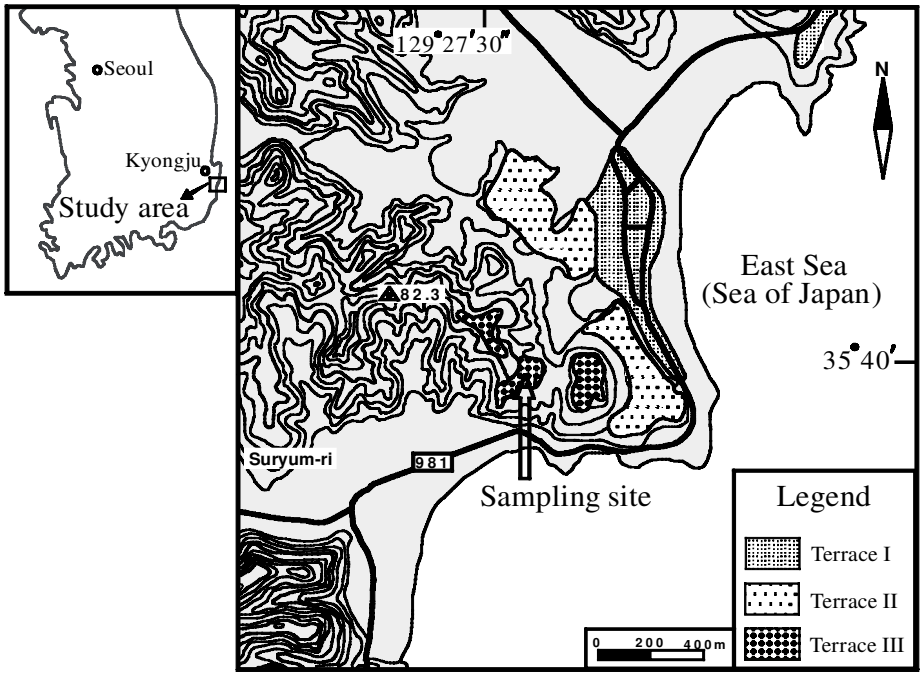

Figure 1. Location of study site and distribution of Quaternary marine terraces (modified from Lee *et al.*, 1999). Interval between contours = 10 m.

elevation of the terrace. The range of their OSL ages was confirmed by one of the present authors (C.S. Cheong, unpublished data). Figure 2 is a sketch of the cross-section of the weathered terrace deposit investigated in detail. The terrace deposit, 2–3 m thick, is composed of thick gravel layers interbedded with two thin sandy gravel layers 3–17 cm thick. Gravel layers consist of well-rounded pebbles of biotite granite, granite porphyry, arkosic sandstones, hornfels, andesite, basalt and andesitic/basaltic tuff. In the sandy gravel layers, the pebbles are scattered in the sandy matrix. The terrace deposits are underlain by Tertiary basaltic lapilli tuff, which originally consisted mostly of basaltic pumices, but was transformed to bentonite via diagenetic alteration. The lapilli tuff contains abundant subhedral plagioclase phenocrysts up to 5 mm in size within pumices or angular plagioclase fragments in the matrix (Figure 3a). The plagioclase was not altered during diagenesis but remains in bentonite.

The terrace deposits were weathered after subaerial exposure. The slope of the study site is ~8°, dipping towards the seashore. The weathering profiles are generally well drained and located above the groundwater table as indicated by their yellow to brown color. The degree of weathering is different between the gravels and the sandy gravel layers. In the gravel layers, most of the pebbles are friable due to intense chemical weathering, and the pores among the pebbles are filled with supergene clays of pale yellowish brown (10YR 6/3) color. However, in the sandy gravels, the pebbles are fresh, and cemented with more dense and rigid supergene clays of yellowish brown (7.5YR 7/2) color. Some of the sand grains in the sandy gravels were completely altered to clay pseudomorphs of grayish yellow (5Y 9/3). The original fabrics of the terrace deposits such as the arrangement and morphology of pebbles almost disappeared in the uppermost portion of the weathering profile with the development of dark reddish brown soil (2.5YR 5/5) (Figure 3b).

SAMPLES AND ANALYTICAL METHODS

Weathered gravels and sandy gravels were sampled extensively from the profiles (Figure 2). Most of the analytical results presented in this paper were obtained from the upper sandy gravel layer, the gravel layer between two sandy layers, the lapilli tuff, and the reddish brown soil (Figure 2). Clay coatings/infillings, pseudomorphs and weathered pebbles were extracted under a stereomicroscope using a steel needle and a surgical blade for detailed mineralogical characterization. X-ray diffraction (XRD) patterns of the extracted clay samples were obtained using a Siemens D5005 instrument equipped with a diffracted-beam monochromator and Cu target. The XRD analyses of poorly crystalline isotropic clays were carried out at the step-scan mode (10 s counting time per 0.02°2θ) using a variable slit system. The thermal properties of the extracted clays were analyzed using a Rigaku TAS100 thermal analyzer with a sample weight of 10 mg and heating rate of 10°C/min in the range 20–1000°C. The extracted clays were dispersed in distilled water and

https://doi.org/10.1346/000986002760832757 Published online by Cambridge University Press

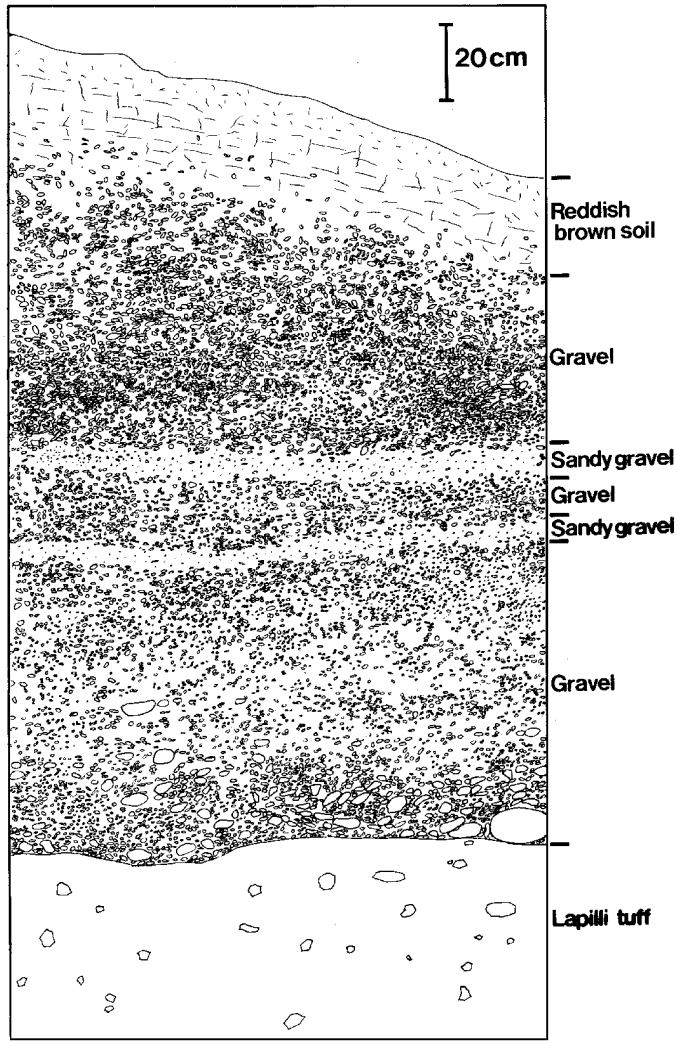

Figure 2. Sketch of the cross-section of the weathered gravel deposits overlying Tertiary lapilli tuff. Note the two thin sandy gravel layers.

loaded on the Cu grid for TEM observation after carbon coating using a Carl Zeiss EM912Ω instrument at an acceleration voltage of 120 kV. Samples of both gravels and sandy gravels were impregnated with epoxy resin diluted with acetone after air drying under vacuum following the method of Jeong and Kim (1993), and thin polished sections were prepared. The volume percentages of clays, mineral fragments and pebbles in the sandy gravel layers were determined by point counting on the thin-sections. Back-scattered electron (BSE) and secondary electron (SE) images were obtained from the thin-sections and untreated samples, respectively, to observe microtextures using a JEOL JSM 6300 scanning electron microscope (SEM) equipped with an Oxford energy dispersive X-ray spectrometer (EDS). The chemical compositions of the minerals were analyzed using a Cameca SX51 electron probe microanalyzer (EPMA) of the Korea Basic Science Institute (operating conditions: acceleration voltage 15 kV, beam current 10 nA, beam diameter 20 μm, counting time 10 s).

RESULTS

Weathered sandy gravels

Photomicrographs of the thin-sections show sandy grains of quartz, plagioclase, pyroxene, rock fragments and pebbles (Figure 3c). Colorless and optically isotropic clays replace plagioclase grains to form pseudomorphs or in part to form reaction rims. In fact, the isotropic clay pseudomorphs are more common than reaction rims, suggesting that most of the plagioclase grains were already replaced by the isotropic clays. The original grains of bytownite are angular to subhedral and range from 0.5 to 2 mm in size. The skeletal plagioclase

https://doi.org/10.1346/000986002760832757 Published online by Cambridge University Press

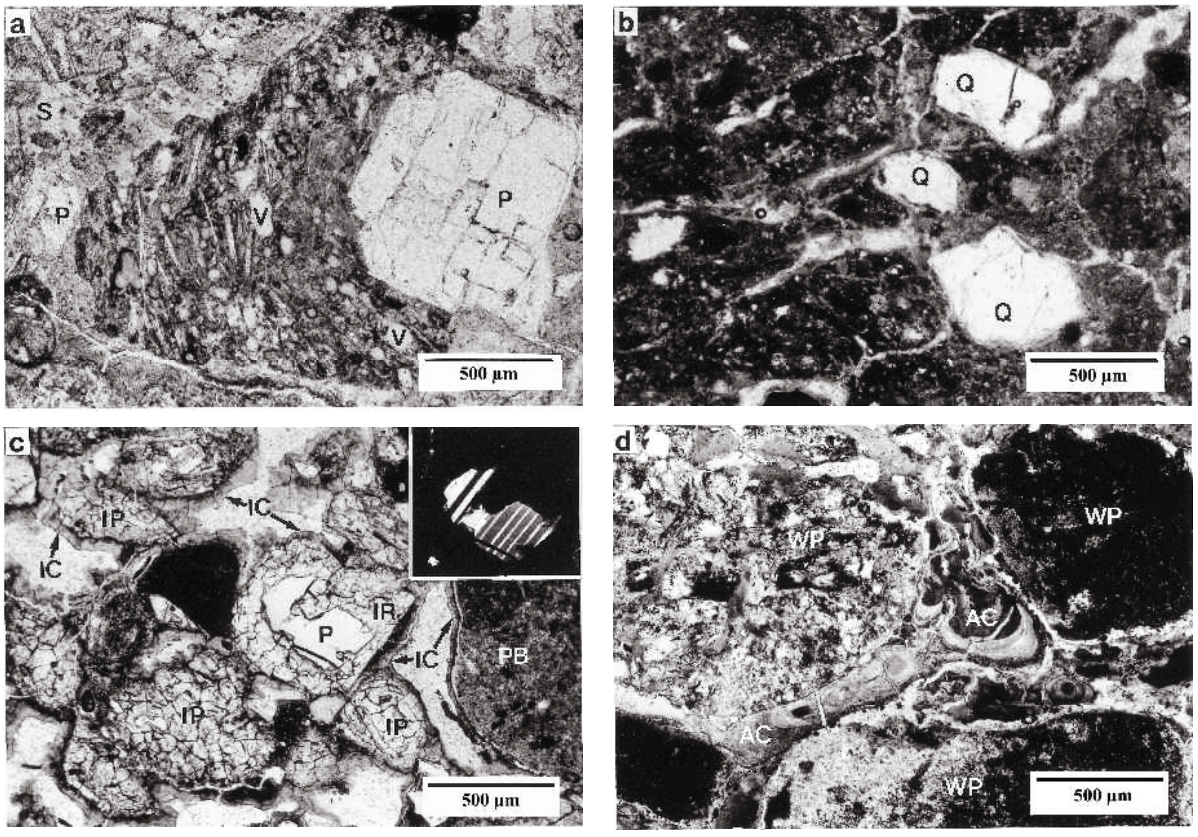

Figure 3. Photomicrographs of thin-sections of lapilli tuff and weathered gravel deposits. (a) Lapilli tuff showing the pumice with vesicles and plagioclase phenocryst in smectite matrix. The vesicles are filled with smectite. (b) Reddish brown soil with no residual texture. (c) Weathered sandy gravel layer showing isotropic clay pseudomorphs, rims replacing plagioclase, and coatings. The inset shows optical isotropism of the clays under cross-polarized light. (d) Weathered gravel layer showing anisotropic clay infillings with convex-downward laminations among weathered pebbles. Photographs under plane-polarized light except the inset. AC: anisotropic clay; IC: isotropic clay coating; IP: isotropic clay pseudomorph; IR: isotropic clay rim; P: plagioclase (bytownite); Q: quartz; PB: pebble; V: vesicle; WP: weathered pebble; S: smectite.

is free of mineral inclusions. Light brown isotropic clays coat sand grains and pebbles throughout the sandy gravel layer. The isotropic clays coat the entire surfaces of sand grains and pebbles in a somewhat regular thickness (10–100 μm) without regard to gravity direction. They do not show lamination due to particulate accumulation. From modal analysis, the weathered sandy gravel is composed of pebble 49.3%, isotropic clay 34.7%, skeletal plagioclase 0.4%, pyroxene 0.5%, quartz 4.9%, and voids 10.2% in volume. About one third of the isotropic clays are pseudomorphic after plagioclase, whereas two thirds coat pebbles and sand grains. Therefore, the original volume of plagioclase is estimated to be 12% from the modal volume of clay pseudomorphs.

A BSE image of a thin-section (Figure 4) shows the detailed microtextures of the isotropic clays replacing plagioclase. The clay rims show regular peripheral distribution around dissolving plagioclase without preferential replacement along the cleavages or microfractures of plagioclase. The isotropic clays have many polygonal desiccation cracks free of translocated clays, probably induced by drying and evacuation during thin-section preparation, suggesting an originally high water content. The EPMA data prove that all the skeletal grains of weathering plagioclase are entirely calcic bytownite (av. An_{86}) (Table 1). For comparison, those of the plagioclase phenocrysts in the underlying Tertiary lapilli tuff are also given in Table 1. The average chemical compositions of the two types of plagioclase are the same within error ranges. The clay pseudomorphs often have cavities at the center and several concentric walls separated by thin narrow pores (Figure 4b). In contrast to bytownite, other sand grains including quartz, K-rich feldspar, pyroxene, and more sodic plagioclase (oligoclase to labradorite) show no significant alteration texture (Figure 4a). Most of the pebbles coated with isotropic clays are not weathered (Figure 4c), but plagioclase laths in the basalt fragments were almost completely transformed to isotropic clay pseudomorphs

https://doi.org/10.1346/000986002760832757 Published online by Cambridge University Press

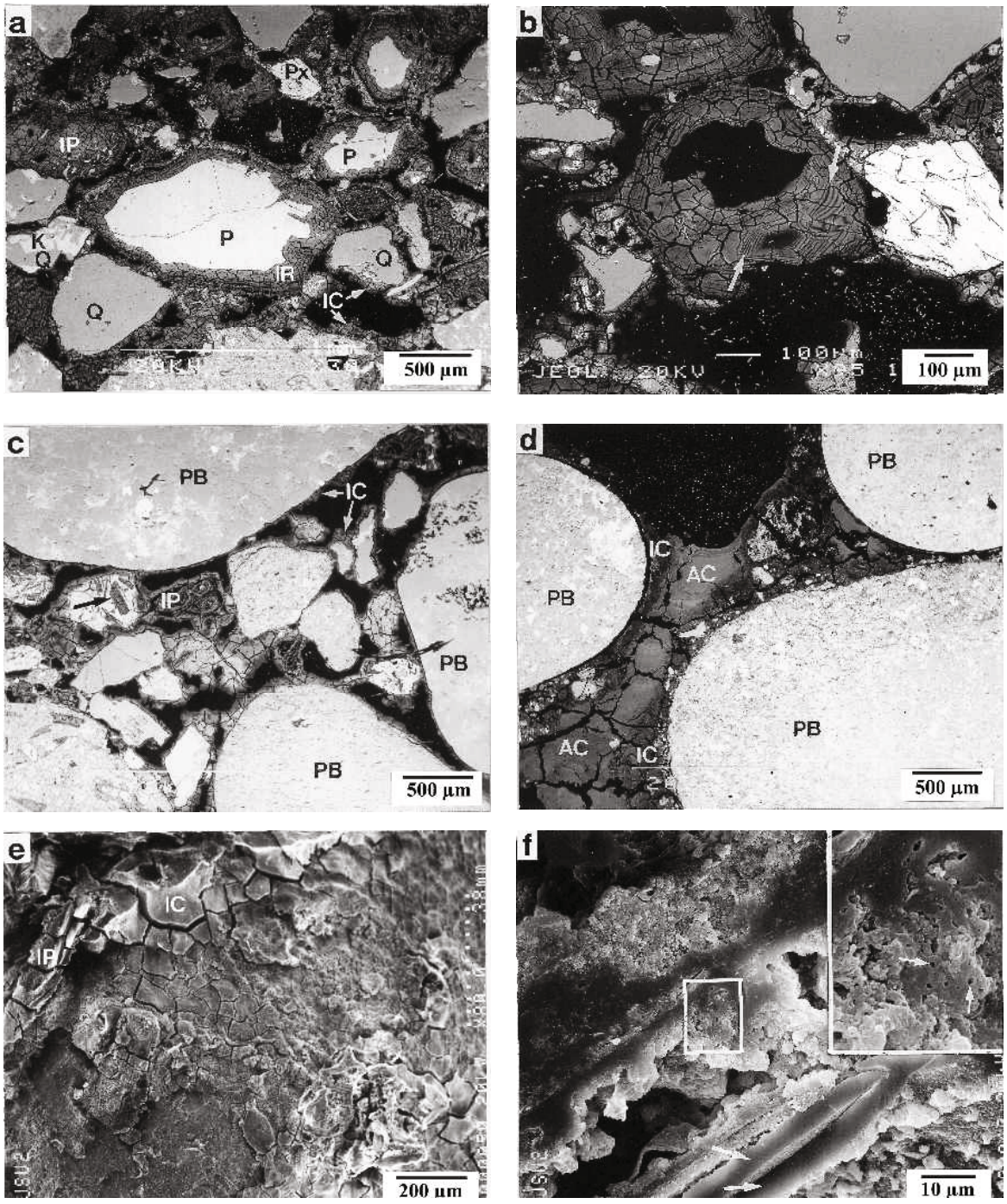

Figure 4. Scanning electron micrographs of the weathered sandy gravel layer. (a) Isotropic clay pseudomorphs, reaction rims enclosing skeletal plagioclase, and coatings. (b) Micrograph magnified from the upper middle of part a showing the cavity at the center of the pseudomorph and the several concentric walls (arrows) separated by narrow pores. Desiccation cracks were developed by drying during sample preparation. (c) The isotropic clays coating sand grains and pebbles with nearly regular thickness. Note the non-weathering of pebbles and the complete alteration of plagioclase to isotropic clays in the basalt grain (black arrow). (d) Non-weathering of pebbles coated with isotropic clays. Note the accumulation of anisotropic clay with convex-downward laminations. (e) The compact isotropic clay aggregates coating the pebbles. (f) The cross-section of an untreated sample of isotropic clay pseudomorph. Note the compact and massive interiors of the isotropic clay walls (arrows) with rugged surfaces. Inset magnified from the box shows hollow circular structures (arrows). (a–d) BSE images of thin-sections, (e–f) SE images of untreated samples. Black: void; K: K-rich feldspar; Px: pyroxene. Other labels are as in Figure 3.

https://doi.org/10.1346/000986002760832757 Published online by Cambridge University Press

Table 1. Electron microprobe analysis of calcic plagioclase (wt.%).

	Sandy gravels (18 grains)		Lapilli tuff (8 grains)	
	Range	Average ($\pm 2\sigma$)	Range	Average ($\pm 2\sigma$)
SiO_2	45.36 –50.00	46.50($\pm$0.55)	44.05 –49.81	45.96($\pm$1.58)
Al_2O_3	30.98 –35.34	33.82($\pm$0.42)	30.06 –34.24	32.84($\pm$1.13)
Fe_2O_3*	0.46 –0.75	0.61($\pm$0.03)	0.43 –0.92	0.61($\pm$0.13)
K_2O	0.00 –0.15	0.03($\pm$0.02)	0.00 –0.05	0.02($\pm$0.01)
Na_2O	1.11 –3.03	1.61($\pm$0.19)	1.15 –3.07	1.73($\pm$0.57)
CaO	14.83 –18.52	17.41($\pm$0.36)	14.85 –18.34	17.33($\pm$1.02)
Total	98.45 –101.28	100.23($\pm$0.30)	97.91 –99.38	98.49($\pm$0.36)
	Mol.%		Mol.%	
Or	0.00 –0.89	0.18($\pm$0.09)	0.00 –0.29	0.1($\pm$0.08)
Ab	9.82 –26.74	14.32($\pm$1.67)	10.20 –27.16	15.3($\pm$5.03)
An	72.37 –90.08	85.50($\pm$1.74)	72.61 –89.78	84.6($\pm$5.09)

* Total Fe as Fe_2O_3

(Figure 4c). The pebbles in the upper interface between gravel and sandy gravel are coated with light brown isotropic clays, and almost unaltered (Figure 4d). The lower part of the voids among the pebbles are filled with yellow brown kaolin clays showing fine laminations that are convex downward (Figure 4d). The EDS analysis of the kaolin infillings showed weak peaks of K, Fe, Ti and Mg, supporting the presence of minor illite or Fe/Ti oxides admixed in the kaolin clay. Iron oxides must have enhanced the brightness of the BSE image compared to isotropic clay coatings.

The SE images of untreated samples show the compact isotropic clay aggregates coating the pebbles (Figure 4e) and the isotropic clay pseudomorphs consisting of several walls (Figure 4f). Their fabrics are highly compact and massive, but their surfaces are very rugged, occasionally with hollow circular structures (Figure 4f).

Mineralogy of isotropic clays

Two diffuse diffraction bands appear at ~3.41 and 2.26 Å in the XRD pattern of the isotropic clay pseudomorph (Figure 5). Despite additional peaks of gibbsite, quartz, augite, plagioclase, and interstratified illite-smectite, the XRD pattern of the isotropic clay coatings also has two broad maxima similar to those in the XRD pattern of the pseudomorph. Impurities were mostly admixed with the isotropic clay coatings during the clay separation process because the isotropic clays were more easily separated from the sand-sized pseudomorph than the thin coatings. The TEM image does not show a distinct morphology but rather continuous gel-like materials with circular voids (Figure 6). The Al/Si atomic ratio of the isotropic clays ranges from 1.3 to 1.7 (av. 1.5) (Table 2). Thermal analysis shows an endothermic peak at 96°C and an exothermic peak at 992°C. The total weight loss is 44.5%, with a large loss of 29.5% up to 226°C and a later gradual loss of 15% up to 918°C (Figure 7).

Weathered gravels

Photomicrographs of the thin-sections show anisotropic clay infillings among weathered pebbles with

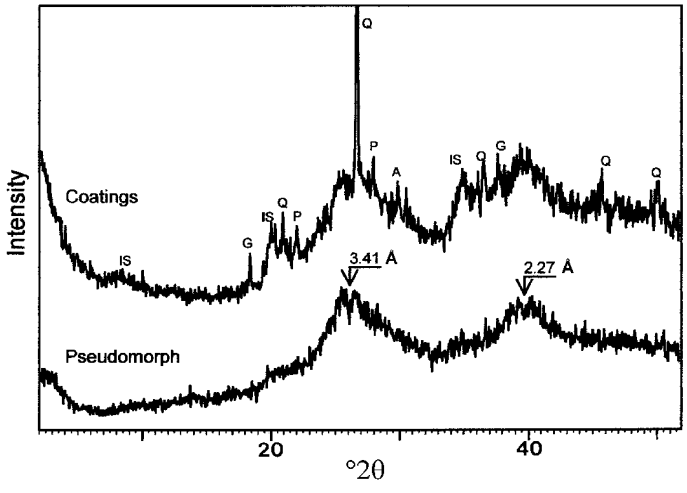

Figure 5. XRD patterns of isotropic clays in the sandy gravel layer. A: augite, G: gibbsite, IS: interstratified illite-smectite, P: plagioclase, Q: quartz. CuKα radiation.

https://doi.org/10.1346/000986002760832757 Published online by Cambridge University Press

concave-upward laminations (Figure 3d). Most of the pebbles in the gravel layer were strongly weathered as shown in the BSE image of Figure 8a. Plagioclases with compositions of albite are replaced by kaolin clays preferentially along the cleavages and microfractures (Figure 8b). Wrinkled kaolin walls were formed along the microfissures. As previously reported from Korea, wrinkled walls are the characteristic fabric of the halloysite aggregates commonly neoforming in the microfissures of weathering plagioclase (Jeong and Kim, 1993; Jeong and Lee, 1998; Jeong, 2000). Biotite was expanded to long vermicular kaolin (Figure 8c), which is a typical morphology for kaolinite transformed from primary mica *via* vermiculite or interstratified mica-vermiculite (Jeong *et al.*, 1995; Jeong, 1998a, 1998b; Jeong, 2000). Micropores in the interior of each pebble formed by the dissolution of constituent minerals are lined with kaolins showing lamination (Figure 8c). From XRD patterns of the weathered pebbles, halloysite, kaolinite and vermiculite are identified as clay minerals (Figure 9). The plagioclase laths in the basalt pebbles were completely removed by dissolution leaving rectangular voids (Figure 8a). Laminated kaolins filling the large pores among the weathered pebbles (Figures 3d and 8a) are identified as halloysite by XRD analysis (Figure 9). The neoformed clays in the weathered pebbles are probably dominated by halloysite in the microfissures of weathering plagioclase with minor kaolinite and vermiculite altered from primary micas. The light reddish brown clays lining/filling the voids

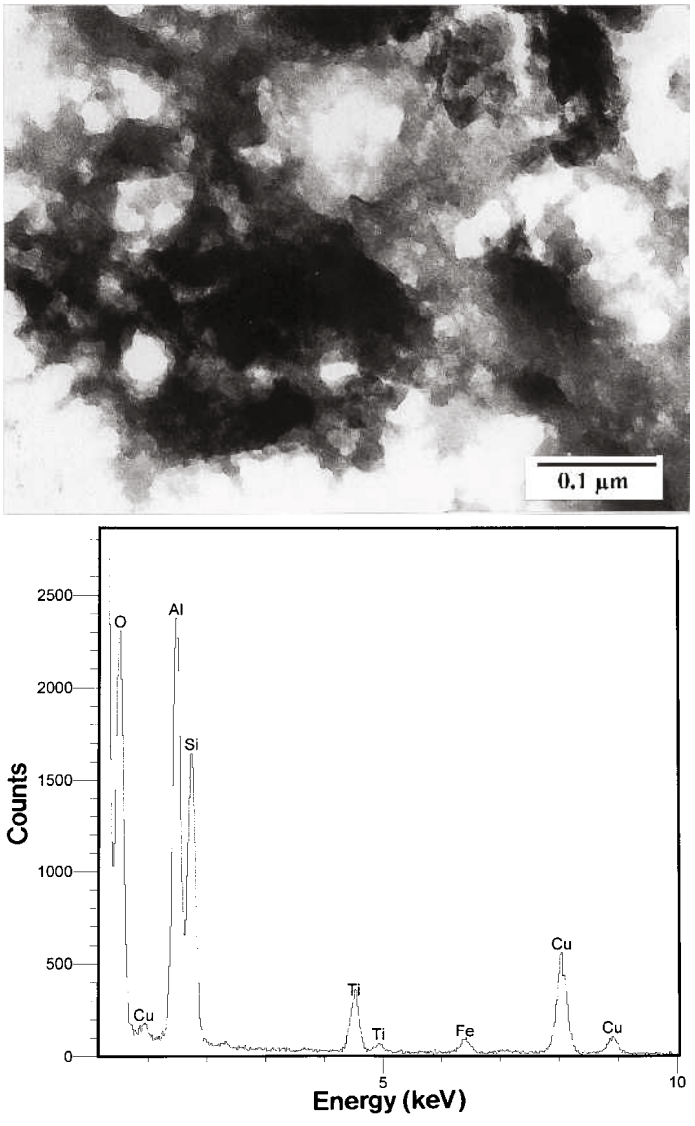

Figure 6. TEM image of the isotropic clay showing gel-like materials with EDS spectrum. The Cu and Ti peaks are ascribed to the Cu grid and holder, respectively.

https://doi.org/10.1346/000986002760832757 Published online by Cambridge University Press

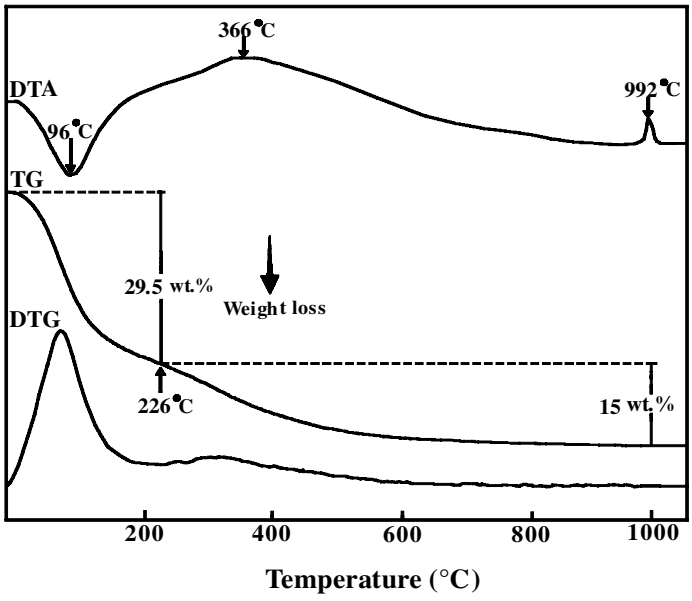

Figure 7. Thermal behavior of the isotropic clay. DTA: differential thermal analysis; TG: thermogravimetry; DTG: differential thermogravimetry.

between the pebbles are mostly halloysite with minor amounts of admixed iron oxides.

DISCUSSION

Mineralogical properties of isotropic clays

Optical isotropism of clays associated with sandy gravel layers is characteristic of amorphous minerals. They consist entirely of Al_2O_3, SiO_2 and H_2O, suggesting allophane or imogolite. Previous works show that the Al/Si atomic ratio of allophane varies between 1 and 2.5, while imogolite is close to 2.0 (Newman and Brown, 1987; Wada, 1989; Childs *et al.*, 1999). Allophane of low Al/Si ratio has a defect kaolin structure, while allophane of high Al/Si ratio, close to 2.0, has an imogolite-like structure called proto-imogolite allophane (Wada, 1989). The average Al/Si ratio of 1.5 is more consistent with previously reported data of allophane than those of imogolite (Wada, 1989). The XRD analysis of allophane showed only two broad diffraction bands at ~3.3 and 2.25 Å, while imogolite displays many peaks in addition to those of allophane (Wada and Yoshinaga, 1969). The XRD pattern of the isotropic clay in this study matches well that of allophane. In the morphological aspect, allophane is known to occur as tiny spheres 30–50 Å in size, but imogolite typically as long fibers (van der Gaast *et al.*, 1985; Wada, 1989). Fibrous or platy morphology typical of crystalline clay minerals was not found by either SEM or TEM observations of the isotropic clays. Their gel-like habit with occasional hollow circular structures (Figures 4f and 6) is closer to the morphology of allophane than that of imogolite presented by Sudo *et al.* (1981) and Eggleton (1987). In the thermal analysis, the first weight loss is ascribed to the adsorbed H_2O, while the second loss may be due to dehydroxylation. Since imogolite has not been identified by XRD, SEM or TEM, the dehydroxylation might reflect the presence of structural OH^- in allophane. In conclusion, the isotropic clays are identified as allophane from the collected mineralogical data described above.

Table 2. Electron microprobe analysis of isotropic clays (26 data points).

	Range	Average ($\pm 2\sigma$)
SiO_2	24.52–34.85	31.24($\pm$1.18)
Al_2O_3	33.28–44.17	39.82($\pm$1.14)
Fe_2O_3*	0.13–1.53	0.52($\pm$0.11)
MgO	0.00–0.32	0.04($\pm$0.03)
MnO	0.00–0.08	0.02($\pm$0.01)
TiO_2	0.00–0.18	0.06($\pm$0.02)
P_2O_5	0.19–1.02	0.4($\pm$0.07)
K_2O	0.00–0.17	0.07($\pm$0.02)
Na_2O	0.00–0.22	0.05($\pm$0.02)
CaO	0.00–0.24	0.1($\pm$0.02)
Total	59.02–79.41	72.33($\pm$2.18)
Al/Si	1.3–1.7	1.5($\pm$0.04)

* Total Fe as Fe_2O_3

Origin of allophane

Although allophane has been reported in weathered basalt (Sieffermann and Millot, 1969) as well as Andisol (Parfitt and Furkert, 1980; Wada, 1989) and Spodosol (Farmer, 1984), its relationship to the primary minerals has rarely been documented on the basis of microscopic

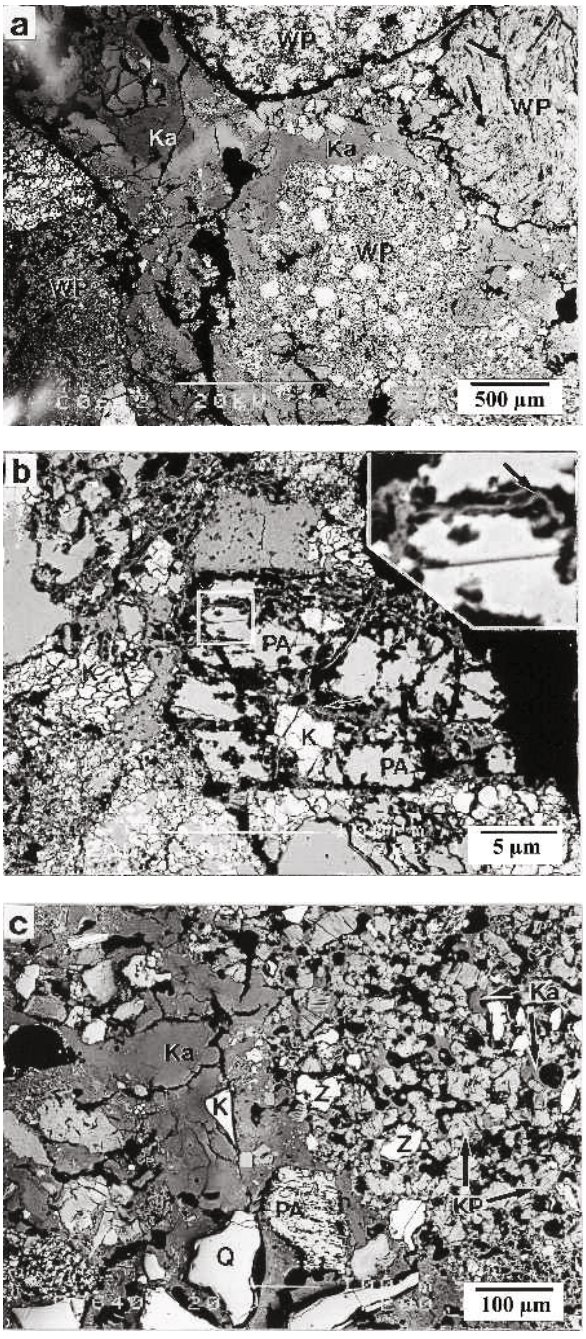

Figure 8. BSE images of thin-sections of the weathered gravel layer. (a) Weathered pebbles and kaolin clay infillings. Arrows indicate the dissolution cavities of plagioclase in a basaltic pebble. (b) Kaolin clay (arrow) formed along the microfissures of plagioclase (albite) in the weathered pebble. The inset image magnified from the box shows the wrinkled kaolin wall (arrow). (c) Weathered pebble showing micropores, pore-lining kaolin clays (Ka with arrows), and expanded kaolinite pseudomorph (KP with arrows) after mica. Black: void; Ka: kaolin infillings among the weathered pebbles; PA: plagioclase (albite); Z: zoisite. Other labels are as in Figure 3.

observations. Previous studies often described the weathering of plagioclase in basalt to kaolin (Nesbitt and Wilson, 1992) and smectite (Bain *et al.*, 1980; Eggleton *et al.*, 1987), but rarely reported the formation of allophane from plagioclase. Jongmans *et al.* (1994) reported the replacement of plagioclase by allophane in the 2C horizon of soil profiles in the Guadeloupe Andisol.

This study presents a clear example of the process of the pseudomorphic replacement of allophane for calcic bytownite (An_{87}). The relative freshness of allophane-coated pebbles in the sandy gravel layers indicates that bytownite weathering and allophane formation occurred prior to pebble weathering. The rapid weathering of bytownite is consistent with Goldich's rule (Goldich, 1938). The dissolution rate of high-Al plagioclase is greater than that of low-Al plagioclase (Welch and Ullman, 1996). The combination of high dissolution rate and high Al/Si ratio of calcic bytownite (An_{87}) resulted in the formation of allophane. In the early stage of weathering, bytownite was dissolved to release solutes like dissolved Al and Si species. The solutes in part precipitated to allophane aggregates at the reaction interface, migrating inward finally to form pseudomorphs after bytownite. However, not all the solutes were used to form allophane pseudomorphs. Despite their compact fabrics, allophane pseudomorphs often have solution cavities in the center and clay walls separated by narrow spaces. Therefore, part of the solutes are mobilized through the solutions wetting the whole surfaces of pebbles and sands, and precipitated to allophane coatings. The fairly uniform thickness of the coatings without regard to gravity direction and the lack of laminations also support their precipitation from solution. From mass balance calculation of the weathered basalt pebbles in Quaternary Allier terraces, Jongmans *et al.* (1993) stated that isotropic clay coating on the weathered basalt pebble was derived from the interior of the pebbles. Allophane coatings in the sandy gravels were not accumulated via particulate translocation through the weathering profiles but neoformed by the weathering of bytownite within the sandy gravel layer.

Confinement of allophane to the bytownite-rich sandy gravel layers indicates that its formation was predominantly controlled by the unique mineralogical make-up of the sandy gravel layers rich in bytownite. The chemical composition, size and morphology of the plagioclase phenocrysts in the Tertiary lapilli tuff are consistent with bytownite in the sandy gravel layers (Table 1). The bytownite sands must have been derived from the underlying lapilli tuff. Since the lapilli tuff was already transformed to bentonite via diagenetic processes, the plagioclase phenocrysts might easily be separated from the smectite matrix in the intense erosional environments of a beach and concentrated in the sandy gravel layers.

https://doi.org/10.1346/000986002760832757 Published online by Cambridge University Press

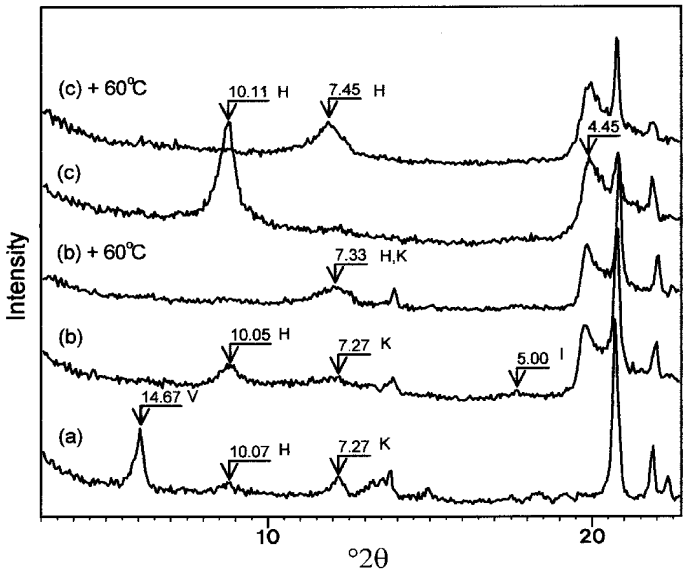

Figure 9. XRD patterns of the weathered materials in the gravel layer. (a) Weathered biotite granite porphyry. (b) Weathered arkosic sandstone pebble. (c) Clay infillings among the weathered pebbles. H: halloysite; I: illite; K: kaolinite; V: vermiculite. The *d*-values are in Å.

Retarded weathering of allophane-coated pebbles

The freshness of allophane-coated pebbles in the sandy gravel layers is contrasted with the highly weathered pebbles in the gravel layers. Allophane has a high water-sorption capacity and a large surface area even compared to smectite (Wada, 1989). Jongmans *et al.* (2000) reported that the stable aggregates of allophane and imogolite indurated the C horizon in the Andisol of Costa Rica derived from andesitic ash. Our SEM and TEM micrographs show that allophane in the sandy gravels occurs as continuous and compact gel-like aggregates rather than as discrete particles. In contrast to the allophane pseudomorphs having central cavities and pores between clay walls, the coatings surrounding pebbles have no visible cavity on the SEM scale. Therefore, the compact allophane gels must have greatly reduced the exchange of weathering solution between pebble and pore. The allophane gels acted as an impermeable geochemical barrier to greatly retard the weathering reaction between pebble and the ambient weathering solution.

In contrast, pebbles in adjacent porous gravel layers have undergone prolonged weathering reaction with solutions. Micropores in the interior of the weathered pebbles were produced by dissolution of plagioclase, and secondary kaolin clays, mostly halloysite, were newly precipitated along the microfissures of the plagioclase. However, halloysitic clay linings/infillings among the weathered pebbles are mostly formed by the accumulation of particles as shown in the concave-upward laminations. The tiny halloysite particles with minor kaolinite and iron oxides were disaggregated by a pedogenic process and transported down the weathered gravel layers along with percolating weathering solutions. The physical accumulation of clay made up of translocated discrete kaolin particles appears to be less effective than the *in situ* chemical precipitate of allophane gel in the retardation of pebble weathering.

Mineral dissolution experiments have been studied extensively to quantify elemental fluxes in global biogeochemical cycles. However, the laboratory weathering rates of minerals are larger than those measured in the field by a few orders of magnitude (Blum and Stillings, 1995). Recent studies suggest that clay coatings may reduce the dissolution rates of minerals (Courchesne *et al.*, 1996; Murakami *et al.*, 1998; Nugent *et al.*, 1998). This study has some implications for the natural weathering rate of rocks and minerals. Rapid weathering of highly soluble bytownite results in the great retardation of the weathering of other rocks and minerals by the formation of geochemical barriers. Minor soluble minerals may protect other major components from weathering, resulting in the great variation of the weathering rates and geochemical circulation of elements in surficial environments.

CONCLUSIONS

Allophane was formed by the weathering of soluble bytownite plagioclase (An_{86}) restricted to thin sandy gravel layers in the gravel deposits of Quaternary marine terrace. Allophane replaced bytownite in a pseudomorphic manner, and coated pebbles and sand grains. Allophane has an Al/Si ratio of av. 1.5 with 45% H_2O, showing a gel-like habit. Bytownite sands, abundant in the sandy gravel layers, originated in the Tertiary basaltic lapilli tuff underlying the gravel deposits. Allophane was formed in the early stage of weathering

after exposure of the terrace deposits, by selectively replacing highly soluble and aluminous bytownite. Coatings of compact allophane gels precipitated from solutions became an impermeable geochemical barrier and greatly retarded the weathering of pebbles in the sandy gravel layers, whereas pebbles in the gravel layers were severely weathered by prolonged weathering reaction to halloysitic clay. In the gravel deposits, bytownite protected the pebbles from weathering, implying that minor soluble minerals might be one of the factors in the natural variation of the rates of weathering of rocks and sediments.

ACKNOWLEDGMENTS

The authors thank S.J. Kim, M.A. Velbel and D.C. Bain for their helpful suggestions and comments. We are grateful to J.H. Noh for assistance with the thermal analysis, S.H. Lee for the electron microprobe analysis, S.H. Yoo for the scanning electron microscopy, and Y.B. Lee for the transmission electron microscopy. This research was supported by Korea Institute of Nuclear Safety.

REFERENCES

Bain, D.C., Ritchie, P.F.S, Clark, D.R. and Duthie, D.M.L. (1980) Geochemistry and mineralogy of weathered basalt from Morvern, Scotland. *Mineralogical Magazine*, **43**, 865–872.

Bockheim, J.G., Kelsey, H.M. and Marshall, J.G. III (1992) Soil development, relative dating, and correlation of late Quaternary marine terraces in southwestern Oregon. *Quaternary Research*, **37**, 60–74.

Blum, A.E. and Stillings, L.L. (1995) Feldspar dissolution kinetics. Pp. 291–351 in: *Chemical Weathering Rates of Silicates* (A.F. White and S.L. Brantley, editors). Reviews in Mineralogy, **31**. Mineralogical Society of America, Washington, D.C.

Childs, C.W., Hayashi, S. and Newman, R.H. (1999) Five-coordinate aluminum in allophane. *Clays and Clay Minerals*, **47**, 64–69.

Courchesne, F., Turmel, M.-C. and Beauchemin, P. (1996) Magnesium and potassium release by weathering in Spodosols: grain surface coating effects. *Soil Science Society of America Journal*, **60**, 1188–1196.

Eggleton, R.A. (1987) Noncrystalline Fe-Si-Al-oxyhydroxides. *Clays and Clay Minerals*, **35**, 29–37.

Eggleton, R.A., Foudoulis, C. and Varkevisser, D. (1987) Weathering of basalt: changes in rock chemistry and mineralogy. *Clays and Clay Minerals*, **35**, 161–169.

Farmer, V.C. (1984) Distribution of allophane and organic matter in podzol B horizons: reply to Buurman and van Reeuwijk. *Journal of Soil Science*, **35**, 453–458.

Feijtel, T.C.J., Jongmans, A.G. and van Doesburg, J.D.J. (1989) Identification of clay coatings in an old Quaternary terrace of the Allier, Limagne, France. *Soil Science Society of America Journal*, **53**, 876–882.

Gaines, R., Skinner, H.C., Foord, E.E., Mason, B. and Rosenzweig, A. (1997) *Dana's New Mineralogy*. John Wiley & Sons, New York, 1819 pp.

Goldich, S.S. (1938) A study in rock weathering. *Journal of Geology*, **46**, 17–58.

Henmi, T. and Wada, K. (1976) Morphology and composition of allophane. *American Mineralogist*, **61**, 379–390.

Jeong, G.Y. (1998a) Formation of vermicular kaolinite from halloysite aggregates in the weathering of plagioclase. *Clays and Clay Minerals*, **46**, 270–279.

Jeong, G.Y. (1998b) Vermicular kaolinite epitactic on primary phyllosilicates in the weathering profiles of anorthosite. *Clays and Clay Minerals*, **46**, 509–520.

Jeong, G.Y. (2000) The dependence of localized crystallization of halloysite and kaolinite on primary minerals in the weathering profile of granite. *Clays and Clay Minerals*, **48**, 196–203.

Jeong, G.Y. and Kim, S.J. (1993) Boxwork fabric of halloysite-rich kaolin formed by weathering of anorthosite in Sancheong area, Korea. *Clays and Clay Minerals*, **41**, 56–65.

Jeong, G.Y. and Lee, B.Y. (1998) Weathering of plagioclase in Palgongsan granite. *Journal of the Geological Society of Korea*, **34**, 44–57.

Jeong, G.Y., Kim, S.J., Kim, Y.H. and Cho, H.G. (1995) Kaolinite formation by weathering of biotite in Sancheong kaolin. *Journal of the Mineralogical Society of Korea*, **8**, 37–45.

Jongmans, A.G., Veldkamp, E., van Breemen, N. and Staritsky, I. (1993) Micromorphological characterization and micro-chemical quantification of weathering in an alkali basalt pebble. *Soil Science Society of America Journal*, **57**, 128–134.

Jongmans, A.G., van Oort, F., Buurman, P., Jaunet, A.M. and van Doesburg, J.D.J. (1994) Morphology, Chemistry and Mineralogy of isotropic aluminosilicate coatings in a Guadeloupe Andisol. *Soil Science Society of America Journal*, **58**, 501–507.

Jongmans, A.G., Verburg, P., Nieuwenhuyse, A. and van Oort, F. (1995) Allophane, imogolite, and gibbsite in coatings in a Costa Rican Andisol. *Geoderma*, **64**, 327–342.

Jongmans, A.G., Denaix, L., van Oort, F. and Nieuwenhuyse, A. (2000) Induration of C horizons by allophane and imogolite in Costa Rican volcanic soils. *Soil Science Society of America Journal*, **64**, 254–262.

Kwon, S.T., Ree, J.H., Park, Y. and Rhodes, E.J. (1999) An active fault in the southeastern Korean peninsula: Evidence from optically stimulated luminescence dating. P. 27 in: *Abstracts with Program of the 54th Annual Meeting of the Geological Society of Korea*, Seosan, Korea.

Langley-Turnbaugh, S.J. and Bockheim, J.G. (1997) Time-dependent changes in pedogenic processes on marine terraces in coastal Oregon. *Soil Science Society of America Journal*, **61**, 1428–1440.

Lee, B.J., Ryoo, C.-R. and Chwae, U. (1999) Quaternary faults in the Yangnam area, Kyongju, Korea. *Journal of the Geological Society of Korea*, **35**, 1–14.

Lee, D.Y. (1985) Quaternary deposits in the coastal fringe of the Korean Peninsula. Ph.D. thesis, Vrije Universiteit, Brussels, 290 pp.

Murakami, T., Kogure, T., Kadohara, H. and Ohnuki, T. (1998) Formation of secondary minerals and its effect on anorthite dissolution. *American Mineralogist*, **83**, 1209–1219.

Newman, A.C.D. and Brown, G. (1987) The chemical constitution of clays. Pp. 1–128 in: *Chemistry of Clays and Clay Minerals* (A.C.D. Newman, editor). Mineralogical Society, London.

Nesbitt, H.W. and Wilson, R.E. (1992) Recent chemical weathering of basalt. *American Journal of Science*, **292**, 740–777.

Nugent, M.A., Brantley, S.L., Pantano, C.G. and Maurice, P.A. (1998) The influence of natural mineral coatings on feldspar weathering. *Nature*, **395**, 588–591.

Parfitt, R.L. and Furkert, R.J. (1980) Identification and structure of two types of allophane from volcanic ash soils and tephra. *Clays and Clay Minerals*, **28**, 328–334.

Parfitt, R.L. and Kimble, J.M. (1989) Conditions of formation

of allophane in soils. *Soil Science Society of America Journal*, **53**, 971–977.

Sieffermann, G. and Millot, G. (1969) Equatorial and tropical weathering of recent basalts from Cameroon: allophanes, halloysite, metahalloysite, kaolinite, and gibbsite. Pp. 417–430 in: *Proceedings of the International Clay Conference, Tokyo* (L. Heller, editor). Israel University Press, Jerusalem.

Sudo, T., Shimoda, S., Yotsumoto, H. and Aita, S. (1981) *Electron Micrographs of Clay Minerals.* Kodansha and Elsevier, Tokyo, 203 pp.

van der Gaast, S.J., Wada, K., Wada, S.-I. and Kakuto, Y. (1985) Small-angle X-ray powder diffraction, morphology, and structure of allophane and imogolite. *Clays and Clay Minerals*, **33**, 237–243.

van Oort, F., Jongmans, A.G. and Jaunet, A.M. (1994) The progression from optical light microscopy to transmission electron microscopy in the study of soils. *Clay Minerals*, **29**, 247–254.

Veldkamp, E., Jongmans, A.G., Feijtel, T.C., Veldkamp, A. and van Breeman, N. (1990) Alkali basalt gravel weathering in Quaternary Allier river terraces, Limagne, France. *Soil Science Society of America Journal*, **54**, 1043–1048.

Wada, K. (1989) Allophane and Imogolite. Pp. 1051–1087 in: *Minerals in Soil Environments* (J.B. Dixon and S.B. Weed, editors). Soil Science Society of America, Madison, Wisconsin, USA.

Wada, K. and Yoshinaga, N. (1969) The structure of imogolite. *American Mineralogist*, **54**, 50–71.

Welch, S.A. and Ullman, W.J. (1996) Feldspar dissolution in acidic and organic solutions: Compositional and pH dependence of dissolution rate. *Geochimica et Cosmochimica Acta*, **60**, 2939–2948.

(*Received 5 March 2001; revised 18 June 2001; Ms. 530*)